SLAC–PUB–5169
June 1990
(T/E)

BOUND VALENCE–QUARK CONTRIBUTIONS TO HADRON STRUCTURE FUNCTIONS*

STANLEY J. BRODSKY

Stanford Linear Accelerator Center,
Stanford University, Stanford, California 94309

and

IVAN SCHMIDT

Stanford Linear Accelerator Center,
Stanford University, Stanford, California 94309

and

Universidad Federico Santa María
Casilla 110–V, Valparaíso, Chile

ABSTRACT

The conventional separation of "valence" and "sea" quark distributions of a hadron implicitly assumes that the quark and anti-quark contributions to the sea are identical in shape, although this cannot be strictly correct due to the exclusion principle. A new separation of "bound valence" and "non–valence" quark distributions of a hadron is proposed which incorporates the Pauli principle and relates the valence component to the wave-functions of the bound-state valence constituents. With this new definition, the non–valence quark distributions correspond to structure functions which would be measured if the valence quarks of the target hadron were charge-less. The bound valence–quark distributions are not singular at small x, thus allowing for the calculation of sum rules and expectation values which would otherwise be divergent.

Submitted to *Physical Review D*

* Work supported in part by Department of Energy contract DE–AC03–76SF00515 (SLAC), and by Fundación Andes and FONDECYT, Chile.

1. INTRODUCTION

Deep inelastic lepton scattering and lepton–pair production experiments measure the light-cone longitudinal momentum distributions $x = (k_q^0 + k_q^z)/(p_H^0 + p_H^z)$ of quarks in hadrons through the relation

$$F_2^H(x, Q^2) = \sum_q e_q^2 x G_{q/H}(x, Q^2). \tag{1}$$

$F_2^H(x, Q^2)$ is the leading–twist structure function at the momentum transfer scale Q, Four–momentum conservation at large Q^2 then leads to the identification $x = x_{Bj} = Q^2/2p \cdot q$. In principle, the distribution functions $G_{q/H}$ could be computed from the bound state solutions of QCD.[1] For example, given the wavefunctions $\psi_{n/H}^{(Q)}(x_i, \vec{k}_{\perp_i}, \lambda_i)$ in the light–cone Fock expansion of the hadronic state, one can write the distribution function in the form[2]

$$G_{q/H}(x, Q^2) = \sum_{n,\lambda_i} \int \prod_i \frac{dx_i d^2 k_{\perp_i}}{16\pi^3} |\psi_{n/H}^{(Q)}(x_i, \vec{k}_{\perp_i}, \lambda_i)|^2 \sum_{b=q} \delta(x_b - x). \tag{2}$$

Here $x_i = k_i^+/p_H^+ = (k_i^0 + k_i^z)/(p_H^0 + p_H^z)$ is the light–cone momentum fraction of each constituent, where $\sum_i x_i = 1$ and $\sum_i k_{\perp_i} = 0$ in each Fock state n. The sum is over all Fock components n and helicities λ_i, integrated over the unconstrained constituent momenta.

An important concept in the description of any bound state is the definition of "valence" constituents. In atomic physics the term "valence electrons" refers to the electrons beyond the closed shells which give an atom its chemical properties. Correspondingly, the term "valence quarks" refers to the quarks which give the bound state hadron its global quantum numbers. In quantum field theory, bound states of fixed particle number do not exist; however, the expansion Eq. (2) allows a consistent definition of the valence quarks of a hadron: the valence quarks appear in each Fock state together with any number of gluons and quark–anti–quark pairs; each component thus has the global quantum numbers of the hadron.

How can one identify the contribution of the valence quarks of the bound state with the phenomenological structure functions? Traditionally, the distribution function $G_{q/H}$ has been separated into "valence" and "sea" contributions:[4] $G_{q/H} = G^{\rm val}_{q/H} + G^{\rm sea}_{q/H}$, where, as an operational definition, one assumes

$$G^{\rm sea}_{q/H}(x, Q^2) = G^{\rm sea}_{\bar{q}/H}(x, Q^2), \qquad (0 < x < 1), \tag{3}$$

and thus $G^{\rm val}_{q/H}(x, Q^2) = G_{q/H}(x, Q^2) - G_{\bar{q}/H}(x, Q^2)$. The assumption of identical quark and anti-quark sea distributions is clearly reasonable for the s and $\bar{s}$ quarks in the proton. However, in the case of the u and d quark contributions to the sea, anti-symmetrization of identical quarks in the higher Fock states implies non-identical q and $\bar{q}$ sea contributions. This is immediately apparent in the case of atomic physics, where Bethe-Heitler pair production in the field of an atom does not give symmetric electron and positron distributions since electron capture is blocked in states where an atomic electron is already present. Similarly in QCD, the $q\bar{q}$ pairs which arise from gluon splitting as in Fig. 1(a) do not have identical quark and anti-quark sea distributions; contributions from interference diagrams such as Fig. 1(b), which arise from the anti–symmetrization of the higher Fock state wavefunctions, must be taken into account. Although the integral of the conventional valence distribution gives correct charge sum rules, such as $\int_0^1 dx (G_{q/H}(x) - G_{\bar{q}/H}(x))$, it can give a misleading reading of the actual momentum distribution of the valence quarks.

The standard definition also has the difficulty that the derived valence quark distributions are apparently singular in the limit $x \to 0$. For example, standard phenomenology indicates that the valence up-quark distribution in the proton behaves as $G^{\rm val}_{u/p} \sim x^{-\alpha_R}$ for small x[3,4] where $\alpha_R \approx 0.5$.[5] This implies that quantities that depend on the $< 1/x >$ moment of the valence distribution diverge. This is the case for the "sigma term" in current algebra and the $J = 0$ fixed pole in Compton scattering.[6] Furthermore, it has been shown[7] that the change in mass of the proton when the quark mass is varied in the light-cone Hamiltonian is given by an extension of the Feynman–Hellmann theorem:

$$\frac{\partial M_p^2}{\partial m_q^2\,(Q^2)} = \int_0^1 \frac{dx}{x}\, G_{q/p}\,(x, Q^2). \tag{4}$$

In principle, this formula allows one to compute the contribution to the proton–neutron mass difference due to the up and down quark masses. However, again, with the standard definition of the valence quark distribution, the integration is undefined at low x. Even more seriously, the expectation value of the light-cone kinetic energy operator

$$\int_0^1 dx\, \frac{< k_\perp^2 > + m^2}{x}\, G_{q/p}(x, Q). \tag{5}$$

is infinite for valence quarks if one uses the traditional definition. There is no apparent way of associating this divergence of the kinetic energy operator with renormalization.[8] Notice that a divergence at $x = 0$ is an ultraviolet infinity for a massive quark, since it implies $k^+ = k^0 + k^z = 0$; *i.e.* $k^z \to -\infty$. A bound state wavefunction would not be expected to have support for arbitrarily large momentum components.

Part of the difficulty with identifying bound state contributions to the proton structure functions is that many physical processes contribute to the deep inelastic lepton–proton cross section: From the perspective of the laboratory or center of mass frame, the virtual photon can scatter out a bound–state quark as in the atomic physics photoelectric process, or the photon can first make a $q\bar{q}$ pair, either of which can interact in the target. As we emphasize here, in such pair-production processes, one must take into account the Pauli principle which forbids creation of a quark in the same state as one already present in the bound state wavefunction. Thus the lepton interacts with quarks which are both *intrinsic* to the proton's bound-state structure, and with quarks which are *extrinsic; i.e.* created in the electron–proton collision itself. Note that such extrinsic processes would occur in electroproduction even if the valence quarks had no charge. Thus much of the phenomena observed in electroproduction at small values of x, such as Regge behavior, sea distributions associated with photon–gluon fusion processes, and shadowing in nuclear structure functions should be identified with the extrinsic interactions, rather than processes directly connected with the proton's bound–state structure.

In this paper we propose a definition of "bound valence–quark" distribution functions that correctly isolates the contribution of the valence constituents which give the hadron its flavor and other global quantum numbers. In this new separation, $G_{q/p}(x,Q^2) = G^{\rm BV}_{q/p}(x,Q^2) + G^{\rm NV}_{q/p}(x,Q^2)$, non-valence quark distributions are identified with the structure functions which would be measured if the valence quarks of the target hadron had zero electro-weak charge. We shall prove that with this new definition the bound valence–quark distributions $G^{\rm BV}_{q/p}(x,Q^2)$ vanish at $x \to 0$, as expected for a bound–state constituent.

2. CONSTRUCTION OF BOUND VALENCE–QUARK DISTRIBUTIONS

In order to construct the bound valence–quark distributions, we imagine a *gedanken*

QCD where, in addition to the usual set of quarks $\{q\} = \{u, d, s, c, b, t\}$, there is another set $\{q_0\} = \{u_0, d_0, s_0, c_0, b_0, t_0\}$ with the same spin, masses, flavor, color, and other quantum numbers, except that their electromagnetic charges are zero.

Let us now consider replacing the target proton p in the lepton–proton scattering experiment by a charge-less proton p_0 which has valence quarks q_0 of zero electromagnetic charge. In this extended QCD the higher Fock wavefunctions of the proton p and the charge-less proton p_0 both contain $q\bar{q}$ and $q_0\bar{q}_0$ pairs. As far as the strong QCD interactions are concerned, the physical proton and the *gedanken* charge-less proton are equivalent.

We define the bound valence–structure function of the proton from the difference between scattering on the physical proton minus the scattering on the charge-less proton, in analogy to an "empty target" subtraction:

$$F_i^{\mathrm{BV}}(x, Q^2) \equiv F_i^p(x, Q^2) - F_i^{p_0}(x, Q^2). \tag{6}$$

The non-valence distribution is thus $F_i^{\mathrm{NV}}(x, Q^2) = F_i^{p_0}(x, Q^2)$. Here the $F_i(x, Q^2)$ ($i = 1, 2$, etc.) are the leading twist structure functions. The situation just described is similar to the atomic physics case, where in order to correctly define photon scattering from a bound electron, one must subtract the cross section on the nucleus alone, without that bound electron present.[9] Physically the nucleus can scatter photons through virtual pair production, and this contribution has to be subtracted from the total cross section. In QCD we cannot construct protons without the valence quarks; thus we need to consider hadrons with charge-less valence constituents.

Notice that the cross section measured in deep inelastic lepton scattering on p_0 is not zero. This is because the incident photon (or vector boson) creates virtual

$q\bar{q}$ pairs which scatter strongly in the gluonic field of the charge-less proton target. In fact at small x the inelastic cross section is dominated by $J = 1$ gluon exchange contributions, and thus the structure functions of the physical and charge-less protons become equal:

$$\lim_{x \to 0} \left[F_i^p(x, Q^2) - F_i^{p_0}(x, Q^2) \right] = 0. \tag{7}$$

In order to isolate a *specific* bound valence–quark distribution $G^{\rm BV}_{q/H}$ for a particular quark flavor q, we consider the difference between scattering on the target hadron H and scattering on an almost identical hadron with that particular valence quark q replaced by q_0. For example, the difference of cross sections $\sigma\left[\ell p(uud) \to \ell' X\right] - \sigma\left[\ell p_0(u u d_0) \to \ell' X\right]$ defines the bound valence down–quark distribution in the proton:

$$e_d^2 \; x \; G^{\rm BV}_{d/p}(x, Q^2) = F_2^{p(uud)}(x, Q^2) - F_2^{p_0(uud_0)}(x, Q^2). \tag{8}$$

Then

$$F^{\rm BV}_{2H}(x, Q^2) = \sum_q e_q^2 x G^{\rm BV}_{q/H}(x, Q^2). \tag{9}$$

Remarkably, as shown in Section 4, the bound valence–quark distribution function $G^{\rm BV}_{q/H}$ vanishes at $x \to 0$; it has neither Pomeron x^{-1} nor Reggeon $x^{-\alpha_R}$ contributions.

Although the *gedanken* subtraction is impossible in the real world, we will show that, nevertheless, the bound valence–distribution can be analytically constrained at small x_{bj}. This opens up the opportunity to extend present phenomenology and relate measured distributions to true bound state wavefunctions.

In the following sections we will analyze both the atomic and hadronic cases, paying particular attention to the high energy regime.

3. ATOMIC CASE

Since it contains the essential features relevant for our discussion, we will first analyze photon scattering from an atomic target. This problem contains an interesting paradox which was first resolved by Goldberger and Low in 1968.[9] Here we give a simple, but explicit, derivation of the main result.

The Kramers–Kronig dispersion relation relates the forward Compton amplitude to the total photo-absorptive cross section[11]

$$f(k) - f(0) = \frac{k^2}{2\pi^2} \int_0^\infty dk' \frac{\sigma(k')}{k'^2 - k^2 - i\epsilon}, \tag{10}$$

where k is the photon energy. One should be able to apply this formula to scattering on a bound electron (e_b) in an atom. However, there is an apparent contradiction. On the one hand, one can explicitly compute the high energy $\gamma e_b \to \gamma e_b$ forward amplitude: it tends to a constant value at $k \to \infty$, the electron Thomson term, $f(k) \to -e^2/m_b^e$, where m_b^e is the effective electron mass corrected for atomic binding.[10] On the other hand, the $\mathcal{O}\ (e^2)$ cross section for the photoelectric effect $\gamma e_b \to e'$ behaves as $\sigma_{\text{photo}} \sim 1/k$ at high energies. But then the dispersion integral in Eq. (10) predicts logarithmic behavior for $f(k)$ at high energy in contradiction to the explicit calculation. Evidently other contributions to the inelastic cross-section cannot resolve this conflict.

This problem was solved[9] by carefully defining what one means by scattering on a bound state electron. For both the elastic Compton amplitude and the inelastic cross section one must subtract the contribution in which the photon scatters off the Coulomb field of the nucleus (empty target subtraction). Thus $\sigma(k)$ in Eq. (10) is really the difference between the total atomic cross section $\sigma_{\mathrm{atom}}(k)$ and the nuclear cross section $\sigma_{\mathrm{nucleus}}(k)$, which is dominated by pair production. We will present a simple proof that the high energy behavior $\sim 1/k$ of the cross sections exactly cancels in this difference, which is a necessary condition for a consistent dispersion relation.

The total cross section for photon scattering on the atom is dominated by two main terms: the photoelectric contribution and e^+e^- pair production, with the produced electron going into a different state than the electron already present in the atom.[12] On the other hand, in the subtraction, pair production in the field of the nucleus is not restricted by the Pauli principle; this cross section contains a contribution where the produced electron goes into the same state as the bound state electron of the atom, plus other terms in which it goes into different states. These last contributions cancel in the difference $\sigma_{\mathrm{atom}} - \sigma_{\mathrm{nucleus}}$. Thus the bound–state electron photo–absorption cross section is the difference between the photoelectric cross section on the atom and the pair production *capture* cross section on the nucleus, where the produced electron is captured in the same state as the original bound state electron: $\sigma_{e_b} = \sigma_{\mathrm{photoelectric}} - \sigma_{\mathrm{capture}}$. This is depicted graphically in Fig. 2.

We next note that the squared amplitude for the capture process $\gamma Z \to e^+ Atom$ is equal, by charge conjugation, to the squared amplitude for $\gamma \bar{Z} \to e^- \bar{\mathrm{Atom}}$. (See Fig. 3.) Furthermore, by crossing symmetry, the (helicity summed) squared amplitude for this last process is equal to the (helicity summed) squared amplitude for $\gamma Atom \to e^- Z$, with p_Z and $(-p_{\mathrm{Atom}})$ interchanged. This is equivalent to the interchange of the Mandelstam variables $s = (p_\gamma + p_Z)^2$ and $u = (p_\gamma - p_{\mathrm{Atom}})^2$. Thus at high photon energies (where $s \simeq -u$), the two cross sections $\sigma_{\mathrm{photoelectric}}$ and $\sigma_{\mathrm{capture}}$ of Fig. 2 cancel, consistent with the Kramers–Kronig relation. In Regge language, the imaginary part of the $J = 0$ Compton amplitude is zero.

The proof we have presented implicitly assumes the equality of the flux factors for the photoelectric process on the atom and the capture process on the nucleus. This is normally a good approximation since the atomic and nuclear masses are almost identical for $M_Z \gg m_e$. However, for finite mass systems such as muonic atoms, the mass of the nucleus and atom are unequal, and the cross sections do not cancel at high energy. The difficulty in this case is that the nucleus does not provide the correct "empty target" subtraction.

However, we can extend the analysis to the general atomic problem by considering hypothetical atoms A_0 consisting of null leptons ℓ_0 with normal electromagnetic and Coulomb interactions with the nucleus but with zero external charge. [In effect, we consider an extended QED with $U(1) \times U(1)$ gauge interactions, where the null lepton has charge $(-1, 0)$, and the normal lepton and nucleus have charges $(-1, -1)$ and (Z, Z), respectively.] The empty target subtraction is defined as the difference between the cross section on the normal atom $A = (Z\ell)$ and the cross section on the null atom $A_0 = (Z\ell_0)$. Since the mass and binding interactions of A and A_0 are identical, the photo–absorption flux factors are the same in both cases.

As in the earlier proof, the matrix element for the photoelectric process on the atom A becomes equal in modulus at high energies with the matrix element for the capture process on the null atom A_0. Note that in the computation of the capture process amplitude, the presence of the spectator lepton ℓ_0 is irrelevant since it remains in the original quantum state (say $1S$): The required matrix element of the current is

$$\left\langle A\ell_0(1S)\ell^+|J^\mu|A_0\right\rangle = \left\langle A\ell_0(1S)\ell^+|\bar{\psi}_\ell\gamma^\mu\psi_\ell b^\dagger_{\ell_0}(1S)|Z\right\rangle = \left\langle A\ell^+|J^\mu|Z\right\rangle .$$

By charge conjugation and crossing this is equal in modulus to

$$\langle Z\ell^- | J^\mu | A \rangle ,$$

the corresponding photoelectric matrix element with $s \to u$. Final–state interactions can only affect the phase at high energies. Thus we obtain cancellation of the photoelectric and capture cross sections at high energies, and verify the Kramers–Kronig dispersion relation for Compton scattering on leptons bound to finite mass nuclei.

4. REGGEON CANCELLATIONS IN QCD

We now return to the analysis of the "bound valence–quark distributions" of the proton. According to the discussion of Section 2, the measurement of the bound valence–quark distribution requires an "empty target" subtraction:

$$\sigma(\gamma^* p \to X) - \sigma(\gamma^* p_0 \to X).$$

For example, in order to specifically isolate the bound valence d–quark distribution of the proton $p(uud)$, we subtract the deep inelastic cross section on the system $p_0(uud_0)$ in which the d_0 valence quark has normal QCD interactions but does not carry electric charge. (Both p and p_0 contain higher Fock states with arbitrary number of gluons, $q\bar{q}$, and $q_0\bar{q}_0$ pairs.) It is clear that the terms associated with $J \approx 1$ Pomeron behavior due to gluon exchange cancel in the difference. In this section we shall prove that the Reggeon terms also cancel, and thus the resulting distribution of bound valence d quarks $G^{\rm BV}_{d/p}(x, Q^2) = \left[[F_2^{p(uud)}(x, Q^2) - F_2^{p_0(uud_0)}(x, Q^2)] / e_d^2 \, x \right]$ vanishes as $x \to 0$.

As in the atomic case, we now proceed to describe the leading contributions to the scattering of a photon from both the proton p and the state p_0. The high Q^2

virtual photo–absorption cross section on the proton (lab frame) contains two types of terms: contributions in which a quark in p absorbs the momentum of the virtual photon; and terms in which a $q\bar{q}$ pair is created, but the produced q is in a different quantum state than the quarks already present in the hadron. On the other hand, the cross section for scattering of the virtual photon from the state $p_0(uud_0)$ contains contributions that differ from the $p(uud)$ case in two important aspects: first the virtual photon can be absorbed only by charged quarks; and in $d\bar{d}$ pair production on the null proton p_0, the d quark can be produced in any state. Thus the difference between the cross sections off p and p_0 equals a term analogous to $\sigma_{\text{photoelectric}}$, in which a d quark in p absorbs the photon momentum, minus a $d\bar{d}$ pair production contribution on p_0 analogous to σ_{capture}, in which the produced d quark ends up in the same quantum state as the d quark in the original proton state p. This is shown graphically in Fig. 4.[13]

Reggeon behavior in the electroproduction cross section can be understood as due to the appearance of a spectrum of bound $q\bar{q}$ states in the t−channel. The absorptive cross section associated with t−channel ladder diagrams is depicted in Fig. 5(a). The summation of such diagrams leads to Reggeon behavior of the deep inelastic structure functions at small x.[14] In the rest system, the virtual photon creates a $d\bar{d}$ pair at a distance proportional to $1/x$ before the target. The radiation which occurs over this distance contributes to the physics of the Reggeon behavior.

A corresponding Reggeon contribution at low x also occurs in the subtraction term indicated in Fig. 5(b). In the case of the proton target, the d−quark, after radiation, cannot appear in the quantum state already occupied by the d−quark in the proton because of the Pauli principle. However, the corresponding contribution is allowed on the p_0 target: in effect, the d–quark replaces the d_0–quark and is captured into a proton. The capture cross section is computed from the amplitude for $\gamma^* p_0 \to \bar{d}^* p \; d_0^{1S}$.[15] As in the corresponding atomic physics analysis, the spectator d_0 quark in the null target p_0 is inert and cancels out from the amplitude. Thus we only need to consider effectively the (helicity summed) squared amplitude for $\gamma^*(uu) \to \bar{d}^* p$. However, as illustrated in Fig. 6 this amplitude, after charge conjugation and crossing $s \to u$, is equal to the (helicity summed) $\gamma^* p \to d^*(uu)$ squared amplitude at small x. The flux factors for the proton and null proton target are equal.

If we write $s\sigma_{\rm photoelectric}$ as a sum of Regge terms of the form $\beta_R |s|^{\alpha_R}$, where $\alpha_R > 0$ then the subtraction of the capture cross section on the null proton will give the net virtual photo–absorption cross section as a sum of terms $s\sigma^{\rm BV} = \sum_R \beta_R (|s|^{\alpha_R} - |u|^{\alpha_R})$. If we ignore mass corrections in leading twist, then $s \simeq Q^2(1-x)/x$ and $u \simeq -Q^2/x$. Thus for small x every Regge term is multiplied by a factor $K_R = (-\alpha_R)x$. For example, for $\alpha_R = 1/2$ (which is the leading even charge–conjugation Reggeon contribution for non–singlet isospin structure functions), $F_2^{p(uud)} - F_2^{p_0(uud_0)} \sim x^{3/2}$. The bound valence–quark non-singlet ($I = 1$) distribution thus has leading behavior $G_{q/H}^{\rm BV} \sim x^{1/2}$ and vanishes for $x \to 0$.

We can also understand this result from symmetry considerations. We have shown from crossing symmetry $G_{q/p}(x, Q^2) - G_{\overline{q}/p_0}(x, Q^2) \to 0$ at low x. Thus the even charge–conjugation Reggeon and Pomeron contributions decouple from the bound valence–quark distributions.

5. CONCLUSIONS

The observation that the deep inelastic lepton–proton cross section is non–zero, even when the quarks in the target hadron carry no charge, implies that we should distinguish two separate contributions to deep inelastic lepton scattering: *intrinsic* (bound-state) and *extrinsic* (non-bound) structure functions. The extrinsic contributions are created by the virtual strong interactions of the lepton itself, and are present even if the quark fields of the target are charge-less. The bound valence–quark distributions, defined by subtracting the distributions for a gedanken "null" hadron with charge-less valence quarks, correctly isolates the valence–quark contributions intrinsic to the bound–state structure of the target. As we have shown, both the Pomeron and leading Reggeon contributions are absent in the bound valence–quark distributions. The leading Regge contributions are thus associated with particles created by the photon–hadron scattering reaction, processes extrinsic to the bound state physics of the target hadron itself. The bound valence–quark distributions are in principle computable by solving the bound state problem in QCD. Sum rules for the proton derived from properties of the hadronic wavefunction thus apply to the bound valence–quark contributions.

The essential reason why the new definition of the bound valence–quark distribution differs from the conventional definition of valence distributions is the Pauli principle: the anti–symmetrization of the bound state wavefunction for states which contain quarks of identical flavor. As we have shown, this effect plays a dynamical role at low x, eliminating leading Regge behavior in the bound valence–quark distributions. In the atomic physics case, where there is no leading Regge behavior, the analogous application of the Pauli principle leads to analytic consistency with the Kramers–Kronig dispersion relation for Compton scattering on a bound electron.

Acknowledgements

We wish to thank J. Bjorken, J. Collins, D. Issler, and M. Burkardt for helpful discussions. IS also thanks the kind hospitality of R. Blankenbecler and the theory group at SLAC.

REFERENCES

1. Structure functions for meson, baryon, and nuclear bound states in QCD in one-space and one-time dimensions have been computed numerically by diagonalizing the light-cone Hamiltonian. See K. Hornbostel, S. J. Brodsky, and H.-C. Pauli, SLAC-PUB-4678 and Phys. Rev. D (1990) (in proof); K. Hornbostel, SLAC-0333, Ph. D. thesis, unpublished (1988); and M. Burkardt, Nucl. Phys. A504, 762 (1989).
2. S. J. Brodsky and G. P. Lepage, Phys. Rev. D22, 2157 (1980). Equation (2) is derived in light-cone gauge $A^+ = 0$.
3. J. Kuti and V. F. Weisskopf, Phys. Rev. D4, 3418 (1971).
4. F. E. Close, *An Introduction to Quarks and Partons*, Academic Press (1979).
5. The position α_R of J-plane singularities in the forward virtual Compton amplitude are Q^2-independent, and thus the non-singlet Reggeon behavior $F_2^{NS}(x, Q^2) \sim x^{1-\alpha_R}$ at $x \to 0$ must be unaffected by QCD evolution. We thank J. Collins for conversations on this point.
6. S. J. Brodsky, F. E. Close and J. F. Gunion, Phys. Rev. D5, 1384 (1972).

7. W. Weisberger, Phys. Rev. D5, 2600 (1972); S. J. Brodsky, F. E. Close and J. F. Gunion, Phys. Rev. D8, 3678 (1973); S. J. Brodsky and I. Schmidt, unpublished. This result assumes that the valence quark mass only appears in the light–cone kinetic energy $\sum(k_\perp^2 + m^2)/x$.

8. One can identify the ultraviolet divergences at $x \to 0$ of Eqs. (4) and (5) for sea quarks with the renormalization of the gluon propagator (which cancels in the proton–neutron mass difference.)

9. M. L. Goldberger and F. E. Low, Phys. Rev. 176, 1778 (1968); see also: T. Erber, Ann. Phys. 6, 319 (1959).

10. We neglect here the $\mathcal{O}(e^6)$ light–by–light scattering contributions to the forward Compton amplitude.

11. For discussion and references see M. Damashek and F. J. Gilman, Phys. Rev. D1, 319 (1970).

12. To leading order in α we can ignore higher order processes in the total cross section such as Compton scattering.

13. We neglect processes higher order in $\alpha_{\rm QED}$ such as pair production in the electromagnetic field of the quark d.

14. For a derivation of the Reggeon contribution to the leading twist structure functions, see P. V. Landshoff, J. C. Polkinghorne and R. Short, Nucl. Phys. B28, 224 (1971), and S. J. Brodsky, F. E. Close, and J. F. Gunion, Phys. Rev. D8, 3678 (1973).

15. As usual we neglect hadronization effects and other final–state interactions at high energies.

Figure Captions

Fig. 1 Structure function contributions from the three–quark plus one pair Fock state of the proton. The $d\bar{d}$ pair in diagram (a) contributes to the sea distribution, but diagram (b) due to anti–symmetrization of the d–quarks cannot be separated uniquely into "valence" versus "sea" parts.

Fig. 2 The bound–electron photo–absorption cross section $\sigma_{\gamma e_b}$ is defined as the difference of $\gamma - Atom$ and $\gamma - Nucleus$ cross sections. This can also be expressed as the difference between the atomic "photoelectric" cross section and the pair production "capture" cross section on the nucleus, but with the produced electron going into the same atomic state as the original bound state electron.

Fig. 3 The helicity-summed squared amplitude for the process $\gamma Z \to e^+ Atom$ is equal, by charge conjugation, to the helicity-summed squared amplitude for $\gamma\bar{Z} \to e^-\overline{\text{Atom}}$, up to a phase. This is also equal by crossing to the helicity-summed squared amplitude for the process $\gamma Atom \to e^- Z$, but with s and u interchanged.

Fig. 4 The bound valence–quark distribution of quark d can be calculated from the difference between (a) the cross section on the state p in which the virtual photon momentum is absorbed by the quark d, and (b) the $d\bar{d}$ pair production cross section in the field of p_0, but with the produced d quark ending in the same state as the d quark in the original proton state p.

Fig. 5 Amplitudes describing Reggeon behavior at small x (a) in electroproduction, and (b) in the subtraction term of Fig. 4(b).

Fig. 6 The helicity-summed squared amplitude for (a) $\gamma^* p \to d(uu)$ is equal, by charge conjugation, to the helicity-summed squared amplitude for the process (b) $\gamma^* \bar{p} \rightarrow \bar{d}(\bar{u}\bar{u})$, up to a phase. This is also equal, by crossing symmetry, to the helicity-summed squared amplitude for (c) $\gamma^*(uu) \rightarrow \bar{d}p$, with s and u interchanged. Thus at high energies the Reggeon contribution from the subtraction term of Fig. 5(b) cancels the Reggeon contribution of Fig. 5(a).

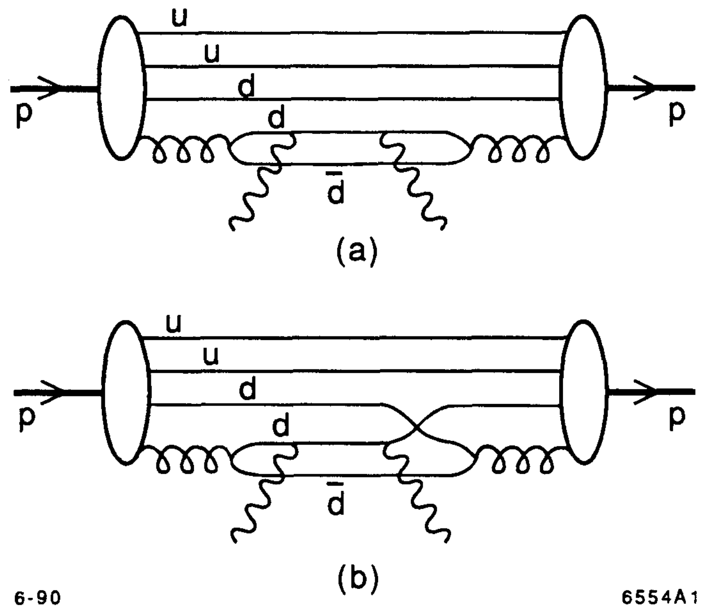

FIGURE 1

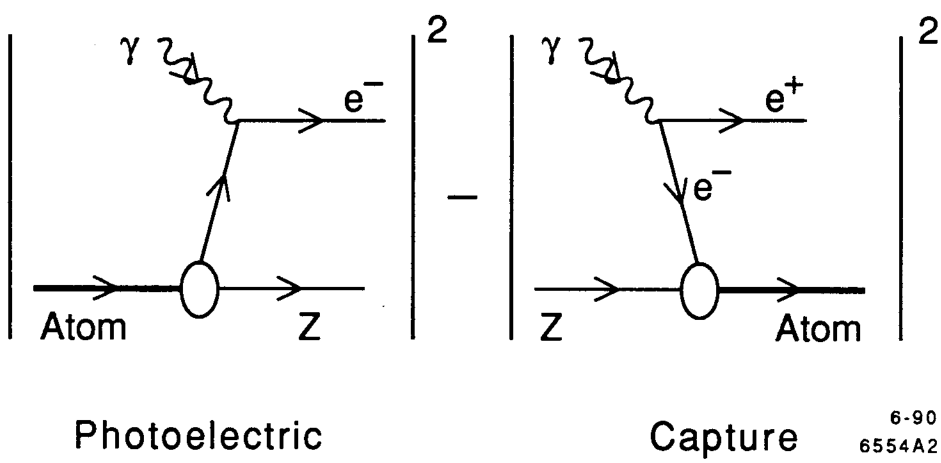

FIGURE 2

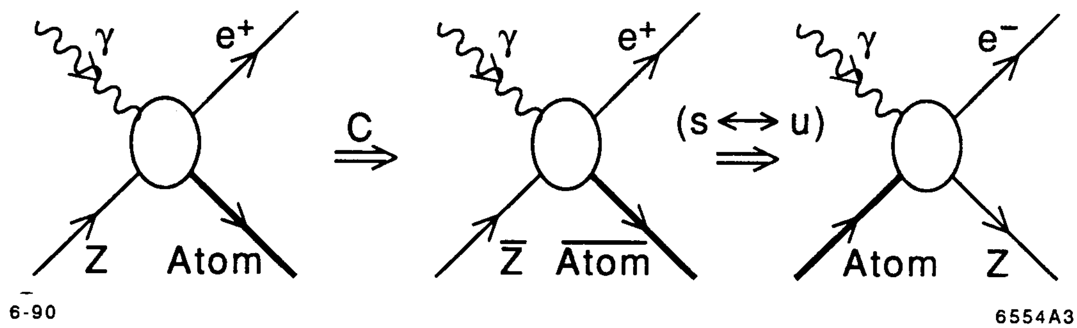

FIGURE 3

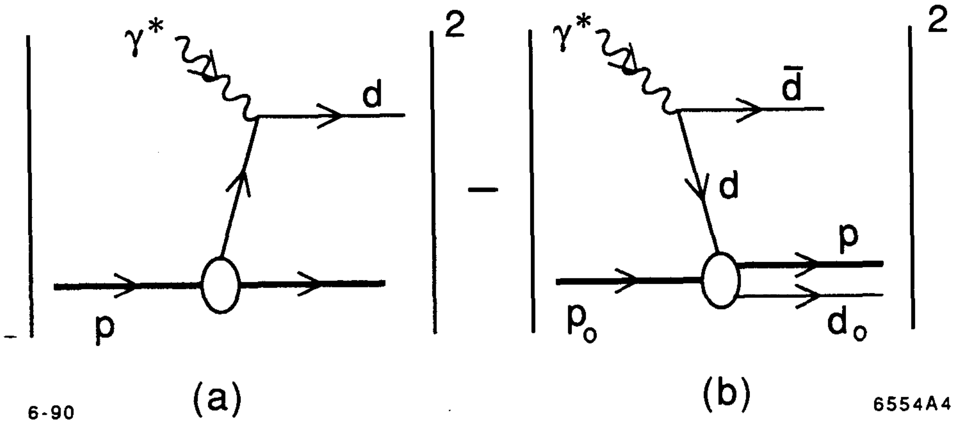

FIGURE 4

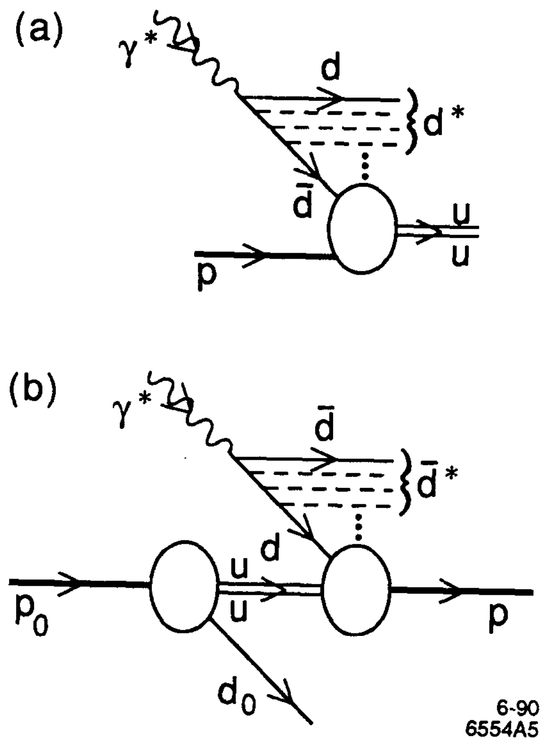

FIGURE 5

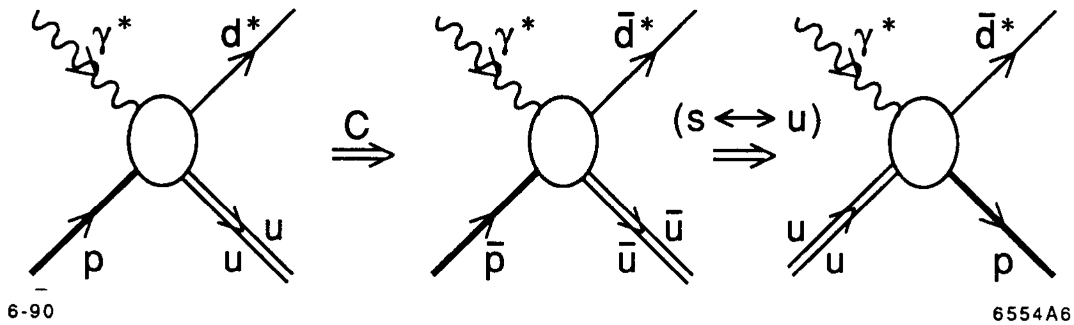

FIGURE 6